Macromolecules
Cite This: Macromolecules 2019, 52, 1308−1316
Article
pubs.acs.org/Macromolecules

# Unraveling Polymer Structures with RAFT Polymerization and Diels−Alder Chemistry

Emily G. Wilborn,[†] Cecilia M. Gregory,[†] Craig A. Machado,[‡] Taylor M. Page,[†] William Ramos,[†] McKenzie A. Hunter,[†] Kiersten M. Smith,[†] Sierra E. Gosting,[†] Roger Tran,[‡] Kim L. Varney,[†] Daniel A. Savin,[‡] and Philip J. Costanzo*[,†]

[†]Department of Chemistry and Biochemistry, California Polytechnic State University, 1 Grand Ave, San Luis Obispo, California 93407-0402, United States

[‡]George & Josephine Butler Polymer Research Laboratory, Center for Macromolecular Science & Engineering, Department of Chemistry, University of Florida, Gainesville, Florida 32611, United States

Supporting Information

**ABSTRACT:** Using Diels−Alders (DA) chemistry as a dynamic-covalent linkage, we explored the kinetic growth mechanism of polymer structures including starlike materials and nanogels. The use of reversible addition−fragmentation chain transfer (RAFT) polymerization allows for precise control of DA linkages within the polymer backbone. Controlling the competition between intra- and intermolecular cross-linking reactions allows for the preparation of polymer structures that can expand their volume after cleavage of the DA linkages as determined by dynamic light scattering (DLS). Macroscopically, this would be analogous to untying a rope ball knot, commonly termed a "monkey's fist".

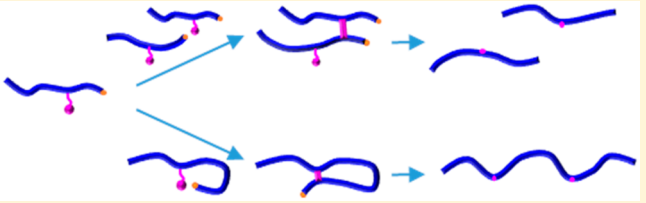

## INTRODUCTION

As synthetic methodologies evolve to become simpler and more efficient, more complex materials, architectures, and structures can be developed and studied. In particular, inspiration from topologically complex polymers, from macroscopic knots to proteins, provides synthetic targets to reproduce.

Fundamentally, topology has been dictated by polymerization methodology or via postpolymerization modification. Polymerization methodologies such as grafting from grafting to grafting through, self-condensing vinyl polymerizations (SCVP), and latent polymerization sites are common techniques to create branched structures. Matyjaszewski et al. have developed a series of polymerization methodologies that can create complex polymer structures in a one-pot methodology.[1−5] Postpolymerization modification approaches have exploited "click" chemistry to implement changes in topology. In particular, the preparation of single chain nanoparticles (SCNPs) has focused on a functional backbone that relies on a secondary cross-linking step.[6−15] Considerable work has also been directed toward controlling the sequence length within polymeric backbones and controlling the polymer topology.[13,16−19] By dictating the sequence length within the polymer backbone, we achieved precise folding and manipulation of the polymer in solution.[13,20,21] Work has advanced beyond simple loop structures, and now complex folding of polymers analogous to enzymes are being synthesized and evaluated.[6,8]

Some of these "click" chemistries have been utilized for their dynamic-covalent properties. Dynamic-covalent linkages also impart some aspects of reversibility that allow bonds to be broken and re-formed on different time scales. For example, boronic esters, oxime formation, and Diels−Alder (DA) chemistry are highly efficient and reversible. Specifically, the preparation of self-healing and rehealable materials using these dynamic-covalent reactions has received extensive attention.[22−27]

DA chemistry has been studied extensively, and the chemical reaction mechanisms are well understood.[28,29] In a DA reaction, a dienophile and a diene undergo a 4 + 2 cycloaddition to form a six-membered ring. The electronic configurations of the diene and dienophile dictate the thermodynamic parameters for both the formation and cleavage of the ring structure. Figure 1 displays one of the most common examples between furan and maleimide. Among

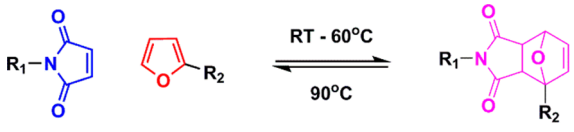


**Figure 1.** Reversible Diels−Alder adduct which has a temperature-dependent formation.

**Received:** September 13, 2018
**Revised:** January 14, 2019
**Published:** January 31, 2019

Downloaded via CALIFORNIA POLY SAN LUIS OBISPO on April 4, 2019 at 22:35:52 (UTC).
See https://pubs.acs.org/sharingguidelines for options on how to legitimately share published articles.

ACS Publications © 2019 American Chemical Society



DOI: 10.1021/acs.macromol.8b01967
Macromolecules 2019, 52, 1308−1316

**Scheme 1. Synthetic Route for Preparation of DA-Xlink**[a]

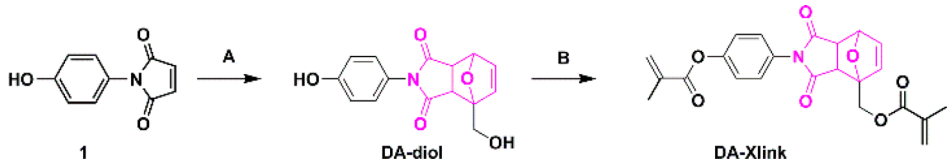


[a]Reagents and conditions: (A) furfuryl alcohol, ACN, 45 °C, 24 h; (B) methacryloyl chloride, DMAP, $Et_3N$, ACN, RT, 24 h.

the various diene−dienophile DA chemistry pairs, many have been used to prepare responsive materials and surfaces.[30−57] For example, many groups have prepared polymer matrices completely composed of DA linkages.[30,40,42,49,56,57] These materials have been mainly exploited as thermally responsive materials for applications in self-healing.[58]

In previous studies, a base polymer was functionalized via chain-end or side-chain to contain DA linkages.[38,48,50,53,55−57] The material is then exploited for its unique rheological profile by exhibiting a large change in viscosity over a narrow temperature window due to the cleavage of DA linkages. DA systems have also been specifically incorporated as a tool to disassemble polymer systems to probe the kinetic growth mechanism of polymers with nonlinear topology.[59,60]

In this work, we aimed to create starlike structures containing Diels−Alder linkages at the core and then to disassemble them to explore the kinetic growth mechanism. During the polymerization, there is constant competition between intra- and intermolecular cross-linking reactions toward the formation of nanogel/starlike structures (NG/SL). In an ideal case, heat treatment would unravel the structures and result in linear polymers; however, we observed the formation of a mixture of morphologies which we propose to include starlike polymers, single chain nanoparticles, and nanogels.

## EXPERIMENTAL SECTION

**Methods and Materials.** All materials were purchased from commercially available sources. $^1$H NMR spectra were recorded on a 400 MHz Varian instrument in *d*-acetone, *d*-DMSO, or $CDCl_3$. Chemical shifts, $\delta$ (ppm), were referenced to the residual solvent signal. *N*-Isopropylacrylamide (NIPAM) was recrystallized in hexanes. Phenolic maleimide (**1**)[58] and 2-(2-carboxyethylsulfanylthiocarbonylsulfanyl)propionic acid (CTA)[61] were synthesized according to previously reported literature.

**Preparation of 4-(Hydroxymethyl)-2-(4-hydroxyphenyl)-3*a*,4,7,7*a*-tetrahydro-1*H*-4,7-epoxyisoindole-1,3(2*H*)-dione (DA-diol).** A 500 mL round-bottom flask was equipped with a stir bar and charged with phenolic maleimide (10.1 g, 53.4 mmol) and acetonitrile (20 mL). The reaction flask was heated to 45 °C, and furfuryl alcohol (5.04 mL, 58.0 mmol) was added. The reaction mixture was stirred for 24 h to yield DA-diol as a tan precipitate (46%, 7.06 g). $^1$H NMR (DMSO): 3.18 (s, 1H), 3.53 (s, 1H), 3.97−4.04 (m, 2H), 5.16 (s, 1H), 5.33 (s,1H), 6.47 (s,1H), 6.81 (ddd, 2H), 6.88 (ddd, 2H).

**Preparation of 4-(4-((Methacryloyloxy)methyl)-1,3-dioxo-1,3,3*a*,4,7,7*a*-hexahydro-2*H*-4,7-epoxyisoindol-2-yl)phenyl Methacrylate (DA-Xlink).** A 250 mL round-bottom flask was equipped with a stir bar and charged with DA-diol (5.00 g, 17.5 mmol) and acetonitrile (150 mL). Triethylamine (5.61 mL, 40.2 mmol) and a catalytic amount of (dimethylamino)pyridine (DMAP) (42 mg) were added to the reaction flask, which was then cooled to 0 °C. Methacryloyl chloride (3.80 mL, 38.4 mmol) was added dropwise. The reaction mixture was stirred for ∼5 h, and completion was indicated by a single TLC spot in 75% ethyl acetate:25% heptane. Solvent was removed via rotary evaporation. The resulting solid was then dissolved in dichloromethane and washed (1 × 1 M HCl, 2 × sat. $NaHCO_3$, 1 × brine). The organic layer was dried with anhydrous $MgSO_4$ and filtered. Solvent was removed via rotary evaporation to yield DA-Xlink as a tan solid (96%, 7.18 g). $^1$H NMR (400 MHz, DMSO): 1.91 (s, 3H), 2.01 (s, 3H), 3.67, (s, 1H), 4.70 (s, 1H), 4.83 (s, 1H), 6.10 (s, 1H), 6.30 (s, 1H), 6.63 (dd, 1H), 6.69 (dd, 1H), 5.41 (s, 1H), 7.22 (ddd, 2H), 7.28 (ddd, 2H).

**Typical Polymerization Conditions.** NIPAM (100−300 equiv) and CTA (1 equiv) were added to a Schlenk flask (50 mL) with a stir bar, and the flask was cooled with a brine/ice bath. V-70 (0.25 EQ) was then quickly added to the Schlenk flask. The flask was sealed with a rubber septum and vacuumed/backfilled with nitrogen (×3) while remaining in a brine/ice bath. Toluene and tetrahydrofuran (THF) were both purged with nitrogen and cooled in ice baths. Using a purged syringe, we added toluene (1 mL, an internal standard) and THF (3−5 mL) to the reaction mixture. The mixture was stirred until all solids dissolved. Once homogeneous, a sample was taken using a purged syringe for analysis by $^1$H NMR. The flask was then placed in an oil bath at 35 °C. The reaction was allowed to polymerize for 1−2 h depending on the desired monomer consumption. Using a purged syringe, we took a kinetic sample. Within moments, DMF (1−4 mL) and a DA-Xlink (1−10 equiv) stock solution in DMF that were previously purged separately were added to the reaction mixture via a purged syringe. The reaction mixture continued to stir at 35 °C for another 4−6 h to reach the desired final conversion. The reaction flask was opened to air to stop the polymerization. A final sample of the reaction mixture was taken, and the remaining solution was added dropwise to stirring diethyl ether to precipitate the polymer. The polymer was collected using vacuum filtration. $^1$H NMR was utilized to calculate percent conversion of NIPAM before addition of the DA-Xlink and of the final reaction. Table S1 lists all reaction conditions in terms of concentration.

**Preparation of Light Scattering Samples.** Polymer (5 mg) was added to a small vial, to which ultrapure water (1 mL) was added, and the vial was vortexed to dissolve polymer. *Note: not all polymer samples were fully soluble. Some samples had insoluble, macroscopically cross-linked pieces.* Aqueous solutions were filtered through either a 0.45 $\mu$m poly(vinylidene fluoride) or a 0.22 $\mu$m poly(ether sulfone) syringe filter into a clean borosilicate cuvette. Heat-treated samples were stirred at 100 °C for 2 h and chilled in cool water before being analyzed once more.

**Dynamic Light Scattering (DLS).** Multiangle DLS analysis was performed on an ALV/CGS-3 four-angle, compact goniometer system (Langen, Germany), which consisted of a 22 mW HeNe linear polarized laser operating at a wavelength of $\lambda$ = 632.8 nm and scattering angles from $\theta$ = 30° to 150°.

Fluctuations in the scattering intensity were measured via an ALV/LSE-5004 multiple tau digital correlator and analyzed via the intensity autocorrelation function ($g^{(2)}(\tau)$). Decay rates, $\Gamma$, were obtained from single-exponential fits using a second-order cumulant analysis, and the mutual diffusion coefficient, $D_m$, was calculated through the relation

$$\Gamma = q^2 D_m$$

where $q^2$ is the scalar magnitude of the scattering vector. The hydrodynamic radius ($R_h$) was calculated through the Stokes−Einstein equation

$$D_m \approx D_0 = \frac{k_B T}{6\pi\eta_s R_h}$$



DOI: 10.1021/acs.macromol.8b01967
*Macromolecules* 2019, 52, 1308−1316

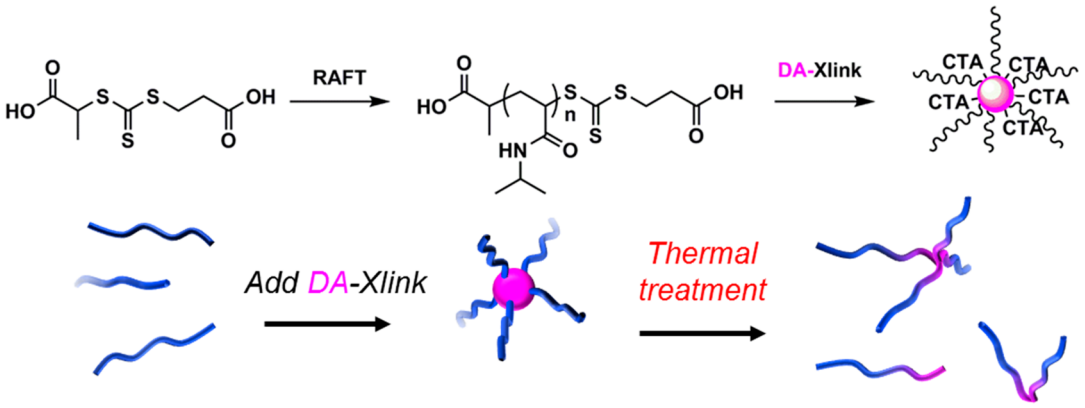


**Figure 2.** Top: synthetic route for preparation of starlike structures. Bottom: schematic representation of assembly and cleavage of starlike structures.

where $D_m$ is approximately equal to the self-diffusion coefficient, $D_0$, $k_B$ is the Boltzmann constant, $T$ is the absolute temperature, and $\eta_s$ is the solvent viscosity.

## RESULTS AND DISCUSSION

**Synthesis of DA-Xlink and Polymers.** Scheme 1 details the preparation of the DA-Xlink. Briefly, phenolic maleimide was treated with furfuryl alcohol in acetonitrile at 45 °C. The resulting DA-diol precipitated from solution after 24 h. Secondary yields of DA-diol could be isolated by reducing the solvent volume and allowing the formation of precipitate. Next, DA-diol was treated with methacryloyl chloride in acetonitrile in the presence of triethylamine and (dimethylamino)pyridine to yield DA-Xlink. We specifically chose to employ a dimethacrylate cross-linker to ensure that NG/SL structures would be formed quickly. Using $Q$ and $e$ values from Odian, we calculated reactivity ratios for methyl methacrylate and acrylamide to be 3.4 and 0.29, respectively.[62] While our monomer system is not identical, we expect monomer reactivities to be similar. This is important as previous attempts to synthesize NG/SL structures with NIPAM using RAFT polymerization reported difficulty, which we attribute to the cross-linker and CTA chosen.[63]

Figure 2 provides a schematic of the polymerization methodology and experimental design. Briefly, NIPAM is polymerized via a RAFT mechanism, and DA-Xlink is added at some percent conversion during the polymerization to link linear PNIPAM chains into nanogel and starlike structures. Based on previous work from Matyjaszewski et al.,[2−4] this synthetic design is expected to afford starlike structures with a core composed of DA cross-links. Thermal treatment would then cleave the DA adducts and reduce the starlike structure to its linear components, which would provide insight into the kinetic growth mechanism in terms of competition between intra- versus intermolecular cross-linking. The variables of interest include (1) target degree of polymerization (DP) (as determined by the initial conditions. DP will be correlated to arm length of the star), (2) concentration of NIPAM monomer, (3) concentration of cross-linker, (4) conversion at which cross-linker is added (whereby higher conversion would lead to longer arms in the star,) (5) final conversion at which polymerization is terminated, and (6) conversion upon addition of DA-Xlink (i.e., the percent of conversion that occurred in the presence of cross-linker). We chose to employ dynamic light scattering to measure $\langle R_h \rangle$ of samples before and after heat treatment. This is in contrast to using size exclusion chromatography due to the nonlinear structures and dynamic composition and topology of the materials prepared, which are known to cause complications in size exclusion chromatography (SEC).[64] Specifically, our SEC employs THF as a solvent and is calibrated against linear polystyrene using only a refractive index detector. THF is not a good solvent for PNIPAM samples, and the use of only refractive index limits the ability to properly interpret branched structures. As such, molecular weight values were not included as their accuracy would be highly questionable. SEC traces of all samples are available in the Supporting Information. Comparison of these traces to DLS data further supports the notions that SEC has limitations in measuring branching topologies as well as the impact of solvent on polymer solution structures (i.e., PNIPAM in THF versus $H_2O$).

A master table listing all samples prepared, including synthetic conditions, is available in Table S1. Relevant entries have been provided here for ease of the reader. (Note: all DPs discussed in text are based on initial monomer to CTA ratio, not the final polymer. This is because the final DP is not easily measured for the complicated topologies in this system. All percentages of DA-Xlink are relative to [NIPAM].) As a preliminary control, linear PNIPAM (**19**) was prepared under similar conditions (range of [NIPAM] and percent conversion achieved), but no DA-Xlink was added. An initial $\langle R_h \rangle$ was observed to be 7 nm, and after heat treatment the $\langle R_h \rangle$ displayed a slight increase to 10 nm. This sample was allowed to rest at room temperature for over 2 weeks, and no change in $\langle R_h \rangle$ was observed. The sample was then sonicated for 30 min, and the $\langle R_h \rangle$ was consistent at 10 nm. (Note: during sonication, the PNIPAM was incidentally raised above the LCST due to slightly elevated temperatures from the sonication bath. Samples were cooled in water prior to running DLS.) Completion of an additional heat treatment at 100 °C caused an increase in $\langle R_h \rangle$ to 12 nm. We attribute this small increase in $\langle R_h \rangle$ to irreversible aggregation of NIPAM caused by heating well above the lower critical solution temperature (LCST), which is in agreement with previously reported literature.[65,66] Having observed the behavior of linear NIPAM, NG/SL structures (samples **17** and **18**) were prepared with nonreversible cross-linkers, ethylene glycol dimethacrylate and 1,4-divinylbenzene, respectively. As expected, these samples displayed larger initial $\langle R_h \rangle$ values relative to the linear NIPAM and did not have a significantly different $\langle R_h \rangle$ after heat treatment. The lack of reversible cross-


DOI: 10.1021/acs.macromol.8b01967
Macromolecules 2019, 52, 1308−1316

links in the samples (**17** or **18**) would not allow the structures to be reduced to a more linear topology. Instead, a small increase in $\langle R_h \rangle$ was observed from 10 to 14 nm and 14 to 18 nm for samples **17** and **18**, respectively, which is in agreement with the linear NIPAM sample.

**Table 1. Control Samples Prepared without DA-Xlink**

| | | conversion[b] (%) | | $\langle R_h \rangle$ (nm) | |
|---|---|---|---|---|---|
| sample[a] | cross-linker | before DA-Xlink | final | pre-HT | post-HT |
| **17** | ethylene glycol dimethacrylate[c] | 72 | 76 | 14 | 18 |
| **18** | 1,4-divinylbenzene[d] | 47 | 63 | 10 | 14 |
| **19** | none | n.a. | 65 | 7 | 10 |

[a]Conditions: DP − 200. DP was determined by the initial ratio of monomer to CTA. [b]Conversion determined by $^1$H NMR. [c]2.5% ethylene glycol dimethacrylate cross-linker was added. [d]1.25% divinylbenzene cross-linker was added.

**Effects of Target DP and [DA-Xlink] on Intra- versus Intermolecular Cross-Linking toward Nanogel/Starlike (NG/SL) Formation.** Entries **2**, **14**, and **16** in Table 2 vary the initial DP while holding the percent of DA-Xlink constant at 5.00%. As expected, we observed an increase in the initial $\langle R_h \rangle$ as the DP is increased from 100 to 300. Additionally, we observed a small decrease in the $\langle R_h \rangle$ after heat treatment, indicating a partial cleavage of the core. We had envisioned preparing starlike structures that would reduce to linear components upon heating as what occurred in previous efforts by Sumerlin et al.[59] in the preparation of hyperbranched polymers. As such, all samples should have displayed significant decreases in $\langle R_h \rangle$ after heat treatment if they were reduced to linear polymers of DP in the 100−300 range; however, thermal treatment of the NG/SL structures only displayed moderate decreases. Cleavage of the DA adducts at the core of the starlike structures should result in smaller linear components. However, the polymeric species did not decrease to entirely linear components as the resultant $\langle R_h \rangle$ values are higher than expected for just linear NIPAM. These data indicate the presence of nonreversible cross-links (such as coupling and disproportionation) occurring in the polymerization process, resulting in the formation of nanogels.

**Table 2. Effect of Variation of DP for Preparation of NG/SL Structures**

| | | conversion[c] (%) | | $\langle R_h \rangle$ (nm) | |
|---|---|---|---|---|---|
| sample[a] | DP[b] | before DA-Xlink | final | pre-HT | post-HT |
| **2** | 100 | 62 | 79 | 34 | 28 |
| **14** | 200 | 76 | 84 | 57 | 52 |
| **16** | 300 | 80 | 87 | 99 | 86 |

[a]Conditions: % DA-Xlink = 5.00 mol % relative to [NIPAM]. [b]DP was determined by the initial ratio of monomer to CTA. [c]Conversion determined by $^1$H NMR.

On the basis of ease of experimental design and execution, we chose a DP of 200 as our baseline material and began to explore other variables in the system. Entries **3**−**14** in Table 3 hold the DP constant at 200 and vary the percent of DA-Xlink. Samples with less than 2.5% DA-Xlink displayed only minor increases in $\langle R_h \rangle$ after heat treatment which are attributed to aggregation consistent with the linear NIPAM control. With

**Table 3. Effect of Variation of % DA-Xlink for Preparation of NG/SL Structures**

| | | conversion[c] (%) | | $\langle R_h \rangle$ (nm) | |
|---|---|---|---|---|---|
| sample[a] | % DA-Xlink[b] | before DA-Xlink | final | pre-HT | post-HT |
| **3** | 0.50 | 46 | 83 | 15 | 19 |
| **4** | 0.50 | 64 | 69 | 17 | 20 |
| **5** | 1.25 | 78 | 86 | 15 | 22 |
| **6** | 1.25 | 75 | 86 | 23 | 26 |
| **7** | 2.50 | 70 | 83 | 34 | 69 |
| **8** | 2.50 | 79 | 84 | 40 | 69 |
| **9** | 2.50 | 74 | 85 | 32 | 64 |
| **10** | 2.50 | 75 | 80 | 39 | 54 |
| **11** | 2.50 | 60 | 80 | 35 | 30 |
| **12** | 2.50 | 63 | 72 | 42 | 32 |
| **13** | 5.00 | 74 | 79 | 51 | 35 |
| **14** | 5.00 | 76 | 84 | 57 | 52 |

[a]Conditions: DP − 200. DP was determined by the initial ratio of monomer to CTA. [b]% DA-Xlink is relative to [NIPAM]. [c]Conversion determined by $^1$H NMR.

such a small amount of DA-Xlink present in solution, the possibility of cross-linking is minimal. All samples with >2.5% DA-Xlink displayed a decrease in $\langle R_h \rangle$ after thermal treatment. As previously stated, this was the expected response, as NG/SL structures should be reduced to more linear components after cleavage of the DA adducts. Attempts to employ more than 5% DA-Xlink resulted in significant amounts of cross-linking and gelation. Unexpectedly, samples with 2.5% DA-Xlink displayed an increase or a decrease in $\langle R_h \rangle$ after thermal treatment based on other synthetic factors (*vide infra*). The observed increase in $\langle R_h \rangle$ was unexpected; as such, experiments were repeated by different individuals to confirm reproducibility.

We hypothesize that we prepared nanogels whose cross-link points are composed of a mixture of nonreversible cross-links caused by traditional termination reactions (including disproportionation and coupling) and reversible cross-links composed of DA adducts caused by intramolecular polymerization reactions. We believe a mixture of disproportionation and coupling occurs because of the reactivity ratios of the monomers and the predominant termination modes for methacrylate (disproportionation) and acrylamide (coupling) based monomers. Upon thermal treatment, the DA adducts are cleaved, and the NG/SL structures can unravel, resulting in an increase in $\langle R_h \rangle$. Macroscopically, this would be analogous to unraveling a rope ball knot, also termed a "monkey's fist or paw".[67] Just as the "monkey's fist" exists in an initial dense state, upon untying the knot, the total volume that the rope comprises increases. The NG/SL structures are composed of multitude of polymer chains that can become "untied" upon cleavage of the reversible DA adducts, resulting in the formation of linear and branched polymer chains. Figure 3 displays a schematic representation of the two proposed kinetic growth pathways under these polymerization conditions. Intramolecular events should result in an increase in $\langle R_h \rangle$ after heat treatment while intermolecular events will yield a decrease in $\langle R_h \rangle$ after heat treatment. Chain growth can occur via polymerization of NIPAM or on one side of the DA-Xlink. Once the DA-Xlink is incorporated, there are three potential outcomes for a remaining polymerizable unit. First, it can remain unpolymerized. We believe this is dependent upon the reactions selected and executed. $^1$H NMR analysis of some materials displayed residual vinylic signals (Figures S1 and S2).



DOI: 10.1021/acs.macromol.8b01967
*Macromolecules* 2019, 52, 1308−1316

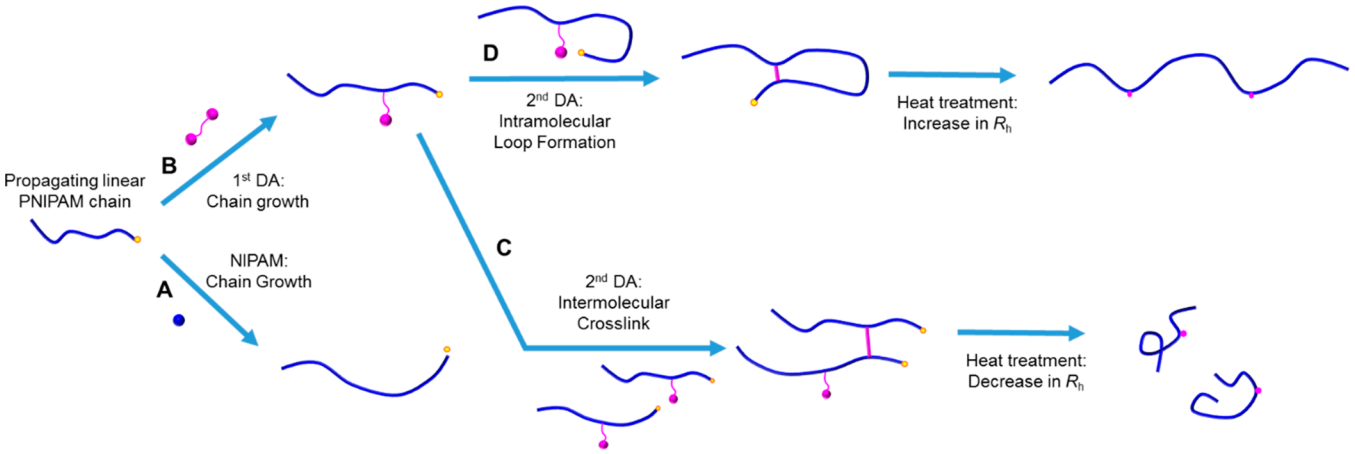


**Figure 3.** Potential pathways for DA-Xlink consumption and the competition between intra- and intermolecular reactions.

Both samples **3** and **4** had 0.5% DA-Xlink; they went to different levels of conversion, and both displayed residual vinylic signals. Other samples had different levels of DA-Xlink and different levels of conversion and did not display any residual vinylic signals.

Once the first vinylic unit is consumed, two pathways are possible. The second possible outcome for the second vinylic unit is an intermolecular reaction can occur between two different polymer chains. Here, a growing polymer chain can polymerize through a pendant DA-Xlink monomer unit on a different chain and join two different polymer chains together. Cleavage of a material with predominantly intermolecular cross-links should yield structures with smaller $\langle R_h \rangle$ values as a single molecule is reduced to several smaller pieces (Figure 3C). The third outcome for the second vinylic unit is an intramolecular reaction can occur. Here, a growing polymer chain can fold upon itself and can create a loop, which would result in a more compact structure. Cleavage of a material with predominantly intramolecular reactions should then produce polymer chains with larger $\langle R_h \rangle$ values (Figure 3D). The trend in our results are qualitatively consistent with these three potential mechanisms when considering concentration of [DA-Xlink].

**Effect of [NIPAM] on Inter- versus Intramolecular Cross-Linking.** It is well-established that competition between intra- and intermolecular reactions can be manipulated by controlling concentration. Comparison of samples **7**, **8**, and **11** focused on how concentration affected the kinetic growth mechanism (Table 4). Samples **7** and **8** had different initial [NIPAM] but were diluted to the same [NIPAM] upon addition of the DA-Xlink. Variation in the $\langle R_h \rangle$ of these samples before thermal treatment can be attributed to the different percent conversion achieved in the reaction, where **7** went to a lower conversion prior to addition of cross-linker and therefore had a smaller $\langle R_h \rangle$. Both samples went to ~83% final conversion and displayed similar $R_h$ after heat treatment. As expected, this indicates that polymerization conditions before the addition of DA-Xlink have little to no effect on the competition between intra- and intermolecular reactions. Samples **7** and **11** had the same initial [NIPAM], but sample **7** was diluted more than **11** upon addition of DA-Xlink. Here sample **7** displayed an increase in $\langle R_h \rangle$ after heat treatment, indicating that intramolecular reactions were dominant during the polymerization. Sample **11** was more concentrated and displayed a decrease in $\langle R_h \rangle$ after heat treatment, indicating that intermolecular reactions were dominant during that polymerization. In more concentrated conditions, polymer chains are closer together, which increases the probability of intermolecular links. When dilute, chains are farther away, which increases the likelihood that the pendant monomer units will be consumed by intramolecular reactions.

**Table 4. Effect of Variation of [NIPAM] for Preparation of NG/SL Structures**

| | [NIPAM] | | conversion[b] (%) | | $\langle R_h \rangle$ (nm) | |
|---|---|---|---|---|---|---|
| sample[a] | initial | final | before DA-Xlink | final | pre-HT | post-HT |
| **7** | 6.09 | 4.44 | 70 | 83 | 34 | 69 |
| **8** | 4.90 | 4.44 | 79 | 84 | 40 | 69 |
| **11** | 6.09 | 5.13 | 60 | 80 | 35 | 30 |

[a]Conditions: DP − 200. DP was determined by the initial ratio of monomer to CTA. % DA-Xlink −2.5%. % DA-Xlink is relative to [NIPAM]. [b]Conversion determined by $^1$H NMR.

**Other Effects on Inter- versus Intramolecular Cross-Linking.** Further analysis of how synthetic conditions can influence intra- versus intermolecular reactions demonstrates how conditions other than [DA-Xlink] or [NIPAM] can influence the system (Table 5). Using 2.5% DA-Xlink as a crossover point for dictating intra- and intermolecular cross-linking, we prepared samples **1** and **15** with a DP of 100 and 300, respectively, with 1.67% DA-Xlink. Analysis of the $R_h$ before and after thermal treatment showed an increase in size for sample **1** and minimal change in size for sample **15**. Moreover, upon comparison of samples **1** and **2**, the higher [DA-Xlink] in sample **1** displayed an increase in $\langle R_h \rangle$ after

**Table 5. Effect of Variation of [NIPAM] for Preparation of NG/SL Structures**

| | | | [NIPAM] | | conversion[c] (%) | | $\langle R_h \rangle$ (nm) | |
|---|---|---|---|---|---|---|---|---|
| sample[a] | DP[b] | % DA-Xlink[c] | initial | final | before DA-Xlink | final | pre-HT | post-HT |
| **1** | 100 | 1.67 | 3.97 | 3.20 | 46 | 82 | 11 | 42 |
| **2** | 100 | 5.00 | 3.71 | 3.03 | 62 | 79 | 34 | 28 |
| **15** | 300 | 1.67 | 7.70 | 6.66 | 67 | 85 | 23 | 23 |
| **16** | 300 | 5.00 | 6.93 | 5.41 | 80 | 87 | 99 | 86 |

[a]DP was determined by the initial ratio of monomer to CTA. [b]% DA-Xlink is relative to [NIPAM]. [c]Conversion determined by $^1$H NMR.



DOI: 10.1021/acs.macromol.8b01967
Macromolecules 2019, 52, 1308−1316

thermal treatment while the more dilute sample **2** displayed a decrease in $\langle R_h \rangle$ after thermal treatment. These comparisons show that the ratio of DA-Xlink to target DP is another key variable in determining intra- versus intermolecular linkages. Finally, looking at the wide range of initial and final [NIPAM] utilized (Table S1), no obvious trend is observed, thus indicating that competition between intra- and intermolecular reactions is influenced by multiple synthetic conditions.

Further analysis of synthetic conditions utilized to prepare samples with 2.5% DA-Xlink provided additional insights into the kinetic growth mechanism (Table 6). In particular, samples

**Table 6. Effect of Percent Conversion in Preparation of NG/SL Structures**

| | [NIPAM] | | conversion[b] (%) | | $\langle R_h \rangle$ (nm) | |
|---|---|---|---|---|---|---|
| sample[a] | initial | final | before DA-Xlink | final | pre-HT | post-HT |
| **7** | 6.09 | 4.44 | 70 | 83 | 34 | 69 |
| **8** | 4.90 | 4.44 | 79 | 84 | 40 | 69 |
| **9** | 5.76 | 3.91 | 74 | 85 | 32 | 64 |
| **10** | 5.76 | 3.49 | 75 | 80 | 39 | 54 |
| **11** | 6.09 | 5.13 | 60 | 80 | 35 | 30 |
| **12** | 6.24 | 4.52 | 63 | 72 | 42 | 32 |

[a]Conditions: DP − 200. DP was determined by the initial ratio of monomer to CTA. % DA-Xlink −2.5%. % DA-Xlink is relative to [NIPAM]. [b]Conversion determined by $^1$H NMR

**7**−**10** achieved at least 69.5% conversion before addition of DA-Xlink occurred, and all samples displayed an increase in $R_h$ after heat treatment. For samples **11** and **12**, DA-Xlink was added at 60% and 63% conversion, respectively, and both displayed a decrease in $\langle R_h \rangle$ after heat treatment. This indicates that the percent conversion at the addition of the DA-Xlink is a key variable.

In total, we have identified the [DA-Xlink], the percent conversion at addition of DA-Xlink, and the window of conversion as key variables in our synthetic system. In an attempt to describe the system in total, we introduce an "effective core concentration" defined as

$$\frac{\text{Arms}}{\text{Star}} \times \text{DA-Xlink}$$

where Arms is calculated by multiplying the percent conversion before addition of DA-Xlink times $[\text{NIPAM}]_{\text{initial}}$, Star is calculated by multiplying the final percent conversion times the $[\text{NIPAM}]_{\text{final}}$, and DA-Xlink is the concentration of DA-Xlink added. This representation correlates the length of the arms relative to the cross-linked core, accounting for the density of cross-links in the core (via DA-Xlink) and the breadth of the conversion window during which cross-linking is possible. Figure 4 plots initial $\langle R_h \rangle$ against the effective core concentration. A general increase in $\langle R_h \rangle$ is observed as the effective core concentration increases, demonstrating the observed effect of [DA-Xlink] on the system. As more DA-Xlink is added, one would expect larger structures to be formed, which is what is observed. Figure S3 displays all samples and includes control samples **17** and **18**, which, as expected, do not fit the same trend. This providing further validation of the observed results. Examining Figure 4 in more detail allows the influence of other components to be revealed.

First, as the window of conversion (represented by the different shapes in Figure 4A) becomes smaller, its effect on the initial $\langle R_h \rangle$ is diminished and other variables dominate. As can be seen by the close proximity of the diamonds (samples **1** and **4**), when the window of conversion is large, the initial $\langle R_h \rangle$ are quite similar. However, the spread in $\langle R_h \rangle$ becomes wider when the window of conversion decreases, as seen with the triangles and squares. Finally, for very low windows of conversion, a large spread can be seen in the circles, indicating other factors are at play. To help the reader, Figure 4B includes only the circles. Adjusting the window of conversion will influence the polymer segment length after incorporation of DA-Xlink, which will ultimately regulate the ability of the growing polymer chain to fold and allow for an intramolecular reactions to occur.

Second, a related trend is observed when interpreting the effect of the percent conversion when the DA-Xlink is added. When the DA-Xlink is added at relatively low conversions (black and blue data points), the $\langle R_h \rangle$ are clustered together. As the percent conversion before addition of the DA-Xlink increases, its effect on the initial $\langle R_h \rangle$ is minimized, and again other variables dominate as demonstrated by the widespread in red symbols. As more monomer is present when the DA-Xlink is added, there is an increased opportunity for the polymer chain to propagate linearly, and the competition between intra- and intermolecular reactions is altered.

In summary, competition between intra- and intermolecular reactions is dictated by the [DA-Xlink], the percent conversion

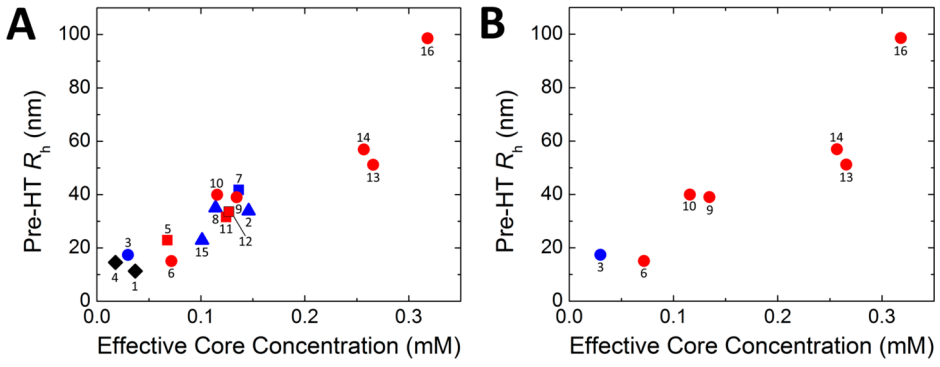


**Figure 4.** Comparison of $\langle R_h \rangle$ (Pre-HT) against the effective kinetic arm length. Symbols and numbers reference entries are in Table S1. (A) Entire data set. (B) Only circles. Symbol description: conversion upon addition of DA-Xlink: (◆) for Δ > 30; (▲) for 15 < Δ < 30; (■) for 9 < Δ < 15; (●) for Δ < 9; see section entitled "Other Effects on Inter- versus Intramolecular Cross-Linking" for more explanation of symbols. Color description: black for $p_x$ < 50, blue for 50 < $p_x$ < 68, and red for $p_x$ > 68, where $p_x$ is the conversion at which DA-Xlink was added.



DOI: 10.1021/acs.macromol.8b01967
*Macromolecules* 2019, 52, 1308−1316

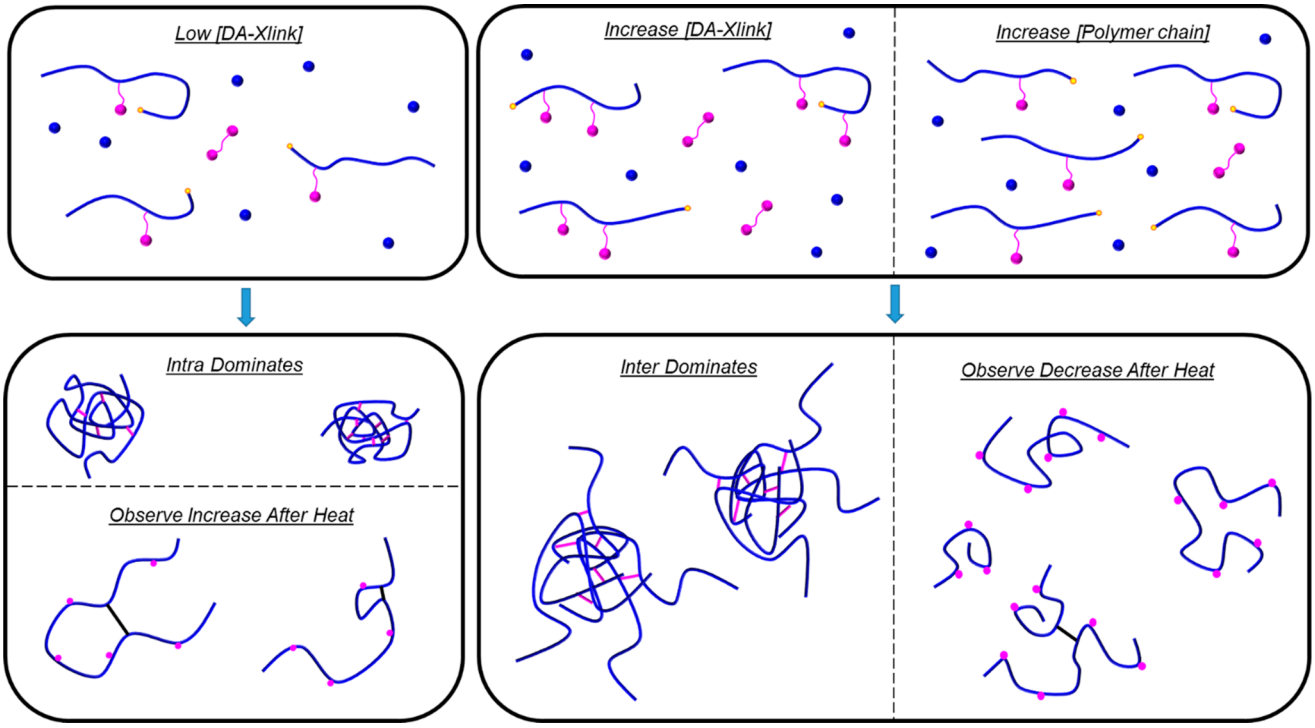


**Figure 5.** Schematic representation of how various experimental conditions influence the competition between intra- and intermolecular reactions.

at addition of DA-Xlink, and the window of conversion, the key variables in our synthetic system. Figure 5 summarizes the various synthetic conditions and the corresponding structures created. At low [DA-Xlink], intramolecular reactions dominate, creating compact structures, and an increase in $\langle R_h \rangle$ is observed after heating. Having a low concentration of DA-Xlink allows for the chain to fold upon itself before an intermolecular event can occur. The percent conversion at the addition of DA-Xlink and the window of conversion will influence growth of the polymer after addition of the DA-Xlink. The segment after incorporation of DA-Xlink must reach a critical length for the polymer chain to have enough flexibility to fold upon itself, and the rate of chain growth must out-compete the probability of an intermolecular event from occurring. By increasing the [DA-Xlink], the incorporation of DA-Xlink is increased, and there are more cross-linkable units on the polymer backbone which will increase the probability of an intermolecular event which results in a decrease in $\langle R_h \rangle$ after heat treatment. Similarly, increasing the concentration of polymer chains will also increase the probability of an intermolecular reaction and a corresponding decrease in $\langle R_h \rangle$ after heat treatment.

## CONCLUSIONS

Polymeric NG/SL structures were prepared using RAFT polymerization with the addition of a difunctional monomer at specific reaction times. By incorporation of DA adducts within the polymer structure, reversible cross-links were incorporated into the material. After heat treatment, the DA adducts were cleaved and the resulting polymeric structures were characterized. Unexpectedly, a range of structures were observed, including materials with larger $\langle R_h \rangle$ as determined by DLS, which we proposed are caused by the unfolding of tightly packed structures. We also propose that a range of non-reversible termination reactions occurred, resulting in non-linear structures. This study elucidates the complex interplay between synthetic factors that determines the topology of NG/SL structures formed by addition of a difunctional monomer. Low cross-linker concentration promotes intramolecular cross-linking events, which leads to more compact structures. However, increasing either the cross-linker content or polymer concentration promotes intermolecular cross-linking events, generating larger NG/SL structures with more constituent polymer chains. This knowledge can be used to gain better control of polymer topology and properties in the future.

## ASSOCIATED CONTENT

### Supporting Information

The Supporting Information is available free of charge on the ACS Publications website at DOI: 10.1021/acs.macromol.8b01967.

$^1$H NMR analysis of various samples; summary table of samples prepared including relevant synthetic conditions (PDF)

## AUTHOR INFORMATION

### Corresponding Author

*E-mail: pcostanz@calpoly.edu; Ph 805-756-2692; Fax 805-756-2692.

### ORCID

Daniel A. Savin: 0000-0002-9235-517X

Philip J. Costanzo: 0000-0001-6220-463X

### Author Contributions

Experiments were performed by E.G.W., C.M.G., C.A.M., T.M.P., W.R., M.A.H., K.A.S., S.E.G., and K.L.V. Data analysis, figure preparation, and writing were completed by E.G.W., C.A.M., P.J.C., and D.A.S. All authors approved the final version and agree to be accountable for the accuracy and integrity of the work.



DOI: 10.1021/acs.macromol.8b01967
*Macromolecules* 2019, 52, 1308−1316

### Author Contributions

E.G.W. and C.M.G. contributed equally.

### Notes

The authors declare no competing financial interest.

## ■ ACKNOWLEDGMENTS

The authors acknowledge the National Science Foundation for support though NSF CHE-1709640 and CHE-1213331 (P.J.C.) as well as CHE-1539347 and DMR-1808204 (D.A.S.).

## ■ REFERENCES

(1) Gao, H.; Matyjaszewski, K. Synthesis of miktoarm star polymers via ATRP using the "In-Out" method: Determination of initiation efficiency of star macroinitiators. *Macromolecules* **2006**, *39*, 7216−7223.

(2) Gao, H.; Matyjaszewski, K. Structural control in ATRP synthesis of star polymers using the arm-first method. *Macromolecules* **2006**, *39*, 3154−3160.

(3) Gao, H.; Matyjaszewski, K. Arm-First Method As a Simple and General Method for Synthesis of Miktoarm Star Copolymers. *J. Am. Chem. Soc.* **2007**, *129*, 11828−11834.

(4) Gao, H.; Matyjaszewski, K. Synthesis of star polymers by a new "core-first" method: sequential polymerization of crosslinker and monomer. *Macromolecules* **2008**, *41* (4), 1118−1125.

(5) Gao, H.; Min, K.; Matyjaszewski, K. Determination of Gel Point during Atom Transfer Radical Copolymerization with Cross-Linker. *Macromolecules* **2007**, *40*, 7763−7770.

(6) Rodriguez, K. J.; Hanlon, A. M.; Lyon, C. K.; Cole, J. P.; Tuten, B. T.; Tooley, C. A.; Berda, E. B.; Pazicni, S. Porphyrin-cored polymer nanoparticles: macromolecular models for heme iron coordination. *Inorg. Chem.* **2016**, *55* (19), 9493−9496.

(7) Lyon, C. K.; Hill, E. O.; Berda, E. B. Zipping polymers into nanoparticles via intrachain alternating radical copolymerization. *Macromol. Chem. Phys.* **2016**, *217* (3), 501−508.

(8) Tooley, C. A.; Pazicni, S.; Berda, E. B. Toward a tunable synthetic [FeFe] hydrogenase mimic:single chain nanoparticles functionalized with a single diiron cluster. *Polym. Chem.* **2015**, *6* (44), 7646−7651.

(9) Cole, J. P.; Lessard, J. J.; Lyon, C. K.; Tuten, B. T.; Berda, E. B. Intra-chain radical chemistry as a route to poly(norbornene imide) single chain nanoparticles: structural considerations and the role of adventitious oxygen. *Polym. Chem.* **2015**, *6* (31), 5555−5559.

(10) Lyon, C. K.; Prasher, A.; Hanlon, A. M.; Tuten, B. T.; Tooley, C. A.; Frank, P. G.; Berda, E. B. A brief user's guide to single-chain nanoparticles. *Polym. Chem.* **2015**, *6* (2), 181−197.

(11) Chao, D.; Jia, X.; Tuten, B. T.; Wang, C.; Berda, E. B. Controlling folding of a novel electroactive polyolefin via multiple sequential orthogonal intra-chain interactions. *Chem. Commun.* **2013**, *49* (39), 4178−4180.

(12) Tuten, B. T.; Chao, D.; Lyon, C. K.; Berda, E. B. Single-chain polymer nanoparticles via reversible disulfide bridges. *Polym. Chem.* **2012**, *3* (11), 3068−3071.

(13) Roy, R. K.; Lutz, J.-F. Compartmentalization of single polymer chains by stepwise intramolecular cross-linking of sequence-controlled macromolecules. *J. Am. Chem. Soc.* **2014**, *136* (37), 12888−12891.

(14) Dirlam, P. T.; Kim, H. J.; Arrington, K. J.; Chung, W. J.; Sahoo, R.; Hill, L. J.; Costanzo, P. J.; Theato, P.; Char, K.; Pyun, J. Single chain polymer nanoparticles via sequential ATRP and oxidative polymerization. *Polym. Chem.* **2013**, *4* (13), 3765−3773.

(15) Hanlon, A. M.; Martin, I.; Bright, E. R.; Chouinard, J.; Rodriguez, K. J.; Patenotte, G. E.; Berda, E. B. Exploring structural effects in single-chain "folding" mediated by intramolecular thermal Diels−Alder chemistry. *Polym. Chem.* **2017**, *8* (34), 5120−5128.

(16) Cavallo, G.; Al Ouahabi, A.; Oswald, L.; Charles, L.; Lutz, J.-F. Orthogonal synthesis of "easy-to-read" information-containing polymers using phosphoramidite and radical coupling sites. *J. Am. Chem. Soc.* **2016**, *138* (30), 9417−9420.

(17) Lutz, J.-F. Coding macromolecules: inputting information in polymers using monomer-based alphabets. *Macromolecules* **2015**, *48* (14), 4759−4767.

(18) Alfurhood, J. A.; Bachler, P. R.; Sumerlin, B. S. Hyperbranched polymers via RAFT self-condensing vinyl polymerization. *Polym. Chem.* **2016**, *7* (20), 3361−3369.

(19) Bachler, P. R.; Forry, K. E.; Sparks, C. A.; Schulz, M. D.; Wagener, K. B.; Sumerlin, B. S. Modular segmented hyperbranched copolymers. *Polym. Chem.* **2016**, *7*, 4155−4159.

(20) Zamfir, M.; Theato, P.; Lutz, J.-F. Controlled folding of polystyrene single chains: design of asymmetric covalent bridges. *Polym. Chem.* **2012**, *3* (7), 1796−1802.

(21) Schmidt, B. V. K. J.; Fechler, N.; Falkenhagen, J.; Lutz, J.-F. Controlled folding of synthetic polymer chains through the formation of positionable covalent bridges. *Nat. Chem.* **2011**, *3* (3), 234−238.

(22) Mukherjee, S.; Hill, M. R.; Sumerlin, B. S. Self-healing hydrogels containing reversible oxime crosslinks. *Soft Matter* **2015**, *11* (30), 6152−6161.

(23) Cash, J. J.; Kubo, T.; Bapat, A.; Sumerlin, B. S. Room-temperature self-healing polymers based on dynamic-covlaent boronic esters. *Macromolecules* **2015**, *48* (7), 2098−2106.

(24) Deng, C. C.; Brooks, W. L. A.; Abboud, K. A.; Sumerlin, B. S. Boronic acid-based hydrogels undergo self-healing at neutral and acidic pH. *ACS Macro Lett.* **2015**, *4* (2), 220−224.

(25) Wojtecki, R. J.; Meador, M. A.; Rowan, S. J. Using the dynamic bond to access macroscopically responsive structurally dynamic polymers. *Nat. Mater.* **2011**, *10* (1), 14−27.

(26) Rowan, S. J.; Cantrill, S. J.; Cousins, G. R.; Sanders, J. K.; Stoddart, J. F. Dynamic covalent chemistry. *Angew. Chem., Int. Ed.* **2002**, *41* (6), 898−952.

(27) Stuart, M. A.; Huck, W. T.; Genzer, J.; Muller, M.; Ober, C.; Stamm, M.; Sukhorukov, G. B.; Szleifer, I.; Tsukruk, V. V.; Urban, M.; Winnik, F.; Zauscher, S.; Luzinov, I.; Minko, S. Emerging applications of stimuli-responsive polymer materials. *Nat. Mater.* **2010**, *9* (2), 101−113.

(28) Carruthers, W. *Cycloaddition Reactions in Organic Synthesis*; Oxford, UK, 1990.

(29) Fringuelli, F.; Taticchi, A. *Dienes in the Diels-Alder Reaction*; John Wiley & Sons: New York, 1990.

(30) Chen, X.; Wudl, F.; Mal, A. K.; Shen, H.; Nutt, S. R. New Thermally Remendable Highly Cross-Linked Polymeric Materials. *Macromolecules* **2003**, *36* (6), 1802−1807.

(31) Costanzo, P. J.; Demaree, J. D.; Beyer, F. L. Controlling Dispersion and Migration of Particulate Additives with Block Copolymers and Diels-Alder Chemistry. *Langmuir* **2006**, *22* (24), 10251−10257.

(32) Costanzo, P. J.; Beyer, F. L. Thermally Driven Assembly of Nanoparticles in Polymer Matrices. *Macromolecules* **2007**, *40* (11), 3996−4001.

(33) Costanzo, P. J.; Beyer, F. L. Thermoresponsive, Optically Active Films Based upon Diels-Alder Chemistry. *Chem. Mater.* **2007**, *19*, 6168−6173.

(34) Dirlam, P. T.; Strange, G. A.; Orlicki, J. A.; Wetzel, E. D.; Costanzo, P. J. Controlling Surface Energy and Wetability with Diels-Alder Chemistry. *Langmuir* **2010**, *26* (6), 3942−3948.

(35) Durmaz, H.; Dag, A.; Altintas, O.; Erdogan, T.; Hizal, G.; Tunca, U. One-Pot Synthesis of ABC Type Triblock Copolymers via in situ Click [3 + 2] and Diels$\hat{*}$*Alder [4 + 2] Reactions. *Macromolecules* **2007**, *40* (2), 191−198.

(36) Gacal, B.; Durmaz, H.; Tasdelen, M. A.; Hizal, G.; Tunca, U.; Yagci, Y.; Demirel, A. L. Anthracene$\hat{*}$*Maleimide-Based Diels$\hat{*}$*Alder *€*Click Chemistry*€* as a Novel Route to Graft Copolymers. *Macromolecules* **2006**, *39* (16), 5330−5336.

(37) Gheneim, R.; Perez-Berumen, C.; Gandini, A. Diels-Alder Reactions with Novel Polymeric Dienes and Dienophiles: Synthesis of Reversibly Cross-linked Elastomers. *Macromolecules* **2002**, *35*, 7246−7253.



DOI: 10.1021/acs.macromol.8b01967
*Macromolecules* 2019, 52, 1308−1316

(38) Goldbach, J. T.; Lavery, K. A.; Penelle, J.; Russell, T. P. Nano- to Macro-sized heterogeneities using cleavable diblock copolymers. *Macromolecules* **2004**, *37* (25), 9639−9645.
(39) Gousse, C.; Gandini, A.; Hodge, P. Application of the Diels$\hat{*}$*Alder Reaction to Polymers Bearing Furan Moieties. 2. Diels$\hat{*}$*Alder and Retro-Diels$\hat{*}$*Alder Reactions Involving Furan Rings in Some Styrene Copolymers. *Macromolecules* **1998**, *31* (2), 314−321.
(40) Heath, W. H.; Palmieri, F.; Adams, J. R.; Long, B. K.; Chute, J.; Holcombe, T. W.; Zieren, S.; Truitt, M. J.; White, J. L.; Willson, C. G. Degradable Cross-Linkers and Strippable Imaging Materials for Step-and-Flash Imprint Lithography. *Macromolecules* **2008**, *41* (3), 719−726.
(41) Imai, Y.; Itoh, H.; Naka, K.; Chujo, Y. Thermally Reversible IPN Organic$\hat{*}$*Inorganic Polymer Hybrids Utilizing the Diels$\hat{*}$*Alder Reaction. *Macromolecules* **2000**, *33* (12), 4343−4346.
(42) Inglis, A. J.; Nebhani, L.; Altintas, O.; Schmidt, F. G.; Barner-Kowollik, C. Rapid Bonding/Debonding on Demand: Reversibly Cross-Linked Functional Polymers via Diels$\hat{*}$*Alder Chemistry. *Macromolecules* **2010**, *43* (13), 5515−5520.
(43) Kavitha, A. A.; Singha, N. K. Smart *€*All Acrylate*€* ABA Triblock Copolymer Bearing Reactive Functionality via Atom Transfer Radical Polymerization (ATRP): Demonstration of a *€*Click Reaction*€* in Thermoreversible Property. *Macromolecules* **2010**, *43* (7), 3193−3205.
(44) Kim, T.-D.; Luo, J.; Tian, Y.; Ka, J.-W.; Tucker, N. M.; Haller, M.; Kang, J.-W.; Jen, A.K.-Y. Diels$\hat{*}$*Alder *€*Click Chemistry*€* for Highly Efficient Electrooptic Polymers. *Macromolecules* **2006**, *39* (5), 1676−1680.
(45) Kosif, I.; Park, E.-J.; Sanyal, R.; Sanyal, A. Fabrication of Maleimide Containing Thiol Reactive Hydrogels via Diels$\hat{*}$*Alder/Retro-Diels$\hat{*}$*Alder Strategy. *Macromolecules* **2010**, *43* (9), 4140−4148.
(46) Luo, K.; Rzayev, J. Living Radical Polymerization of Bicyclic Dienes: Synthesis of Thermally Cross-Linkable Block Copolymers. *Macromolecules* **2009**, *42* (23), 9268−9274.
(47) McElhanon, J. R.; Wheeler, D. R. Thermally responsive dendrons and dendrimers based on reversible furan-maleimide Diels-Alder adducts. *Org. Lett.* **2001**, *3* (17), 2681−2683.
(48) McElhanon, J. R.; Russick, E. M.; Wheeler, D. R.; Loy, D. A.; Aubert, J. H. Removable Foams based on an Epoxy Resin Incorporating reversible Diels-Alder adducts. *J. Appl. Polym. Sci.* **2002**, *85*, 1496−1502.
(49) Murphy, E. B.; Bolanos, E.; Schaffner-Hamann, C.; Wudl, F.; Nutt, S. R.; Auad, M. L. Synthesis and characterization of a single-component thermally remendable polymer network: Staudinger and Stille revisited. *Macromolecules* **2008**, *41*, 5203−5209.
(50) Park, J. O.; Jang, S. H. Synthesis and characterizationof bismaleimides from epoxy resin. *J. Polym. Sci., Part A: Polym. Chem.* **1992**, *30*, 723−729.
(51) Polaske, N. W.; McGrath, D. V.; McElhanon, J. R. Thermally Reversible Dendronized Step-Polymers Based on Sequential Huisgen 1,3-Dipolar Cycloaddition and Diels$\hat{*}$*Alder *€*Click*€* Reactions. *Macromolecules* **2010**, *43* (3), 1270−1276.
(52) Shi, Z.; Luo, J.; Huang, S.; Cheng, Y.-J.; Kim, T.-D.; Polishak, B. M.; Zhou, X.-H.; Tian, Y.; Jang, S.-H.; Knorr, D. B., Jr.; Overney, R. M.; Younkin, T. R.; Jen, A.K.-Y. Controlled Diels$\hat{*}$*Alder Reactions Used To Incorporate Highly Efficient Polyenic Chromophores into Maleimide-Containing Side-Chain Polymers for Electro-Optics. *Macromolecules* **2009**, *42* (7), 2438−2445.
(53) Swanson, J. P.; Rozvadovsky, S.; Seppala, J. E.; Mackay, M. E.; Jensen, R. E.; Costanzo, P. J. Development of Polymeric Phase Change Materials on the basis of Diels-Alder Chemistry. *Macromolecules* **2010**, *43*, 6135−6141.
(54) Szalai, M. L.; McGrath, D. V.; Wheeler, D. R.; Zifer, T.; McElhanon, J. R. Dendrimers based on thermally reversible furan-maleimide Diels-Alder adducts. *Macromolecules* **2007**, *40*, 818−823.
(55) Zhang, Y.; Broekhuis, A. A.; Picchioni, F. Thermally Self-Healing Polymeric Materials: The Next Step to Recycling Thermoset Polymers? *Macromolecules* **2009**, *42* (6), 1906−1912.
(56) Gandini, A.; Silvestre, A. J. D.; Coelho, D. Reversible click chemistry at the service of macromolecular materials. *Polym. Chem.* **2011**, *2*, 1713−1719.
(57) Tasdelen, M. A. Diels-Alder "click" reactions: recent applications in polymer and material science. *Polym. Chem.* **2011**, *2*, 2133−2145.
(58) Amato, N. D.; Strange, G. A.; Swanson, J. P.; Chavez, A. D.; Roy, S. E.; Varney, K. L.; Machado, C. A.; Amato, D. V.; Costanzo, P. J. Synthesis and evaluation of thermally-responsive coatings based upon Diels-Alder chemistry and renewable materials. *Polym. Chem.* **2014**, *5* (1), 69−76.
(59) Sun, H.; Kabb, C.; Sumerlin, B. S. Thermally-labile segmented hyperbranched copolymers: using reversible-covalent chemistry to investigate the mechanism of self-condensing vinyl copolymerization. *Chemical Science* **2014**, *5* (12), 4646−4655.
(60) Bapat, A.; Ray, J. G.; Savin, D. A.; Hoff, E. A.; Patton, D. L.; Sumerlin, B. S. Dynamic-covalent nanostructures prepared by Diels-Alder reactions of styrene-maleic anhydride-derived copolymers obtained by one-step cascade block copolymerization. *Polym. Chem.* **2012**, *3* (11), 3112−3120.
(61) Wang, C.; McCormick, C. L.; Lowe, A. B. Synthesis and evaluation of new dicarboxylic acid functional trithiocarbonates: RAFT synthesis of telechelic poly(n-butyl acrylates)s. *Macromolecules* **2005**, *38*, 9518−9525.
(62) Odian, G. *Principles of Polymerization*; John Wiley and Sons: 2004.
(63) Zheng, G.; Pan, C. Preparation of star polymers based on polystyrene or poly(styrene-b-N-isopropyl acrylamide) and divinyl benzene via reversible addition-fragmentation chain transfer polymerization. *Polymer* **2005**, *46*, 2802−2810.
(64) Peng, Y.; Liu, H.; Zhang, Z.; Liu, S.; Li, Y. Macrocycle-terminated core-cross-linked start polymers: synthesis and characterization. *Macromolecules* **2009**, *42*, 6457−6462.
(65) Lu, Y.; Zhou, K.; Ding, Y.; Zhang, G.; Wu, C. Origin of hysteresis observed in association and dissociation of polymer chains in water. *Phys. Chem. Chem. Phys.* **2010**, *12*, 3188−3194.
(66) Plunkett, K. N.; Zhu, Z.; Moore, J. S.; Leckband, D. E. PNIPAM chain collapse depends on molecular weight and grafting density. *Langmuir* **2006**, *22*, 4259−4266.
(67) Ashley, C. W. *The Ashley Book of Knots*; Doubleday: 1944.



DOI: 10.1021/acs.macromol.8b01967
*Macromolecules* 2019, 52, 1308−1316